

## The effect of SiO<sub>2</sub> nanoparticles content in engine oil on tribological properties of valvetrain chain transmission components

The drive from the crankshaft to the camshaft in an internal combustion engine is usually carried out by means of a cogged belt transmission or a chain transmission when high millage is required without service operations. The valvetrains in CI engines sometimes use the gear transmissions, and the historical rather bevel gear can be found in old cars of collectors or in some motorcycle engines. The chain gear used in SI engines has a two- or three-row chain with high strength, due the unevenness of loads that additionally induce chain pulling and valve timing deregulation. The chain transmission requires the use of pre-tensioners, usually self-acting and driven by springs or oil pressure. The vibrations and chain runout are limited using plastic guides placed on the outside of the long straight sections of the chain. The model of the chain transmission developed with the use of the Finite Elements Method, which operates under oil lubrication conditions, was analyzed. Such the model allowed obtaining weight and mass inertial moments of components. The aim of the study was to evaluate the effect of SiO<sub>2</sub> nanoparticles content in engine oil on the friction between chain transmission components. The resulted values of the friction torque in the chain transmission operating in different conditions of lubrication have been presented in the paper.

Key words: valvetrain, chain transmission, wear, friction, SiO<sub>2</sub> nanoparticles

### 1. Introduction

The combustion engines are commonly used in the most of classic and hybrid vehicles. Their operation is strictly related to the existing valvetrains which can be of cam or camless type. Each cam-type valvetrain contains one or more camshafts. They are driven from the engine crankshaft through a cogged belt transmission or a chain transmission when high millage is required without service operations. The valvetrains in CI engines sometimes use the gear transmissions, and the historical rather bevel gear can be found in old cars of collectors or in some motorcycle engines.

According to [12] chain transmissions are more durable, compact and more efficient than other timing drive systems. If chain dynamics relative to contact stresses, contact forces between various chain drive components exceeds beyond acceptable limits, it leads to vibrations, improper valve and fuel injection timings. Thus, the chain dynamics is the leading source of aggregating Noise, Vibration and Harshness (NVH) issues. If designed valve and injection timings are not achieved, it reduces the volumetric efficiency of the engine and affects overall vehicle performance and fuel economy.

The chain gear used in SI engines contains a one-, two- or three-row chain with high strength, due the unevenness of existing loads during engine operation. Such loads additionally induce chain pulling and can cause valve timing deregulation. The vibrations and chain runout occurring during operation of chain transmission are limited using plastic guides placed on the outside of the long straight sections of the chain. The chain transmission requires the use of pre-tensioners, usually self-acting and driven by springs or drivers using pressure of oil supplied from mean oil line of an engine. Such oil can contain different addi-

tives, i.e. SiO<sub>2</sub> nanoparticles. Components of chain mating with sprockets mounted on camshaft and crankshaft, guides and pretensioner operates under oil lubrication, providing commonly mixture friction conditions. The aim of the study was to evaluate the effect of SiO<sub>2</sub> nanoparticles content in engine oil on the wear and friction of chain transmission components.

### 2. Tribological aspects of the chain transmission

Tribological aspects of the chain transmission are mainly related to the friction torques and friction forces acted on the transmission components and to wear of them. They depend on the engine loading and speed, lubrication conditions and environment parameters, especially temperature, humidity and pollution existence and possibility to reach the interior of transmission.

According [1], the timing drive and valve train generate approx. 20% of overall engine friction losses depending on the engine speed.

According to [14] the friction caused by chain and guide or sprocket rails is mostly higher than in the case of the toothed-belt timing drive. One of main chain drive disadvantages is that the chain drives reach higher noise level than the toothed belt. It is caused by the impact of the chain links on the sprockets. Comparing the life prediction of the two drive mechanisms, the chain timing drive is the best. Chain damages can occur rarely during engine life and the chain timing drive maintenance is not demanding. Regarding timing drive installations there are no high differences associated with using a toothed belt or chain drive.

Pedersen [17] elaborated the simulation model of the dynamics of roller chain drives using a continuous contact force method. The model of the contact surface between the rollers and sprocket was an important issue regarding the

numerical stability of the simulation program and a model with a real tooth profile proved superior to other applied models. With this model it is possible to perform a dynamic simulation of large marine engine chain drives.

Conwell and Johnson [2] created a new test machine configuration providing more realistic chain loading and allowing link tension and roller-sprocket impact monitoring during normal operation.

Pereira et al. [19] used a multibody methodology to address the kinematic and dynamic effects of roller chain drives was presented. The chain itself was modelled as a collection of rigid bodies, connected to each other by revolute clearance joints. Each clearance revolute joint, representing the connection between pair of links, was made up of the pin link/bushing link plus the bushing link/roller pairs, in case of a roller chain. The problem of contact initialization and its coordination with the numerical integration procedures was treated through controlling the time step size of the numerical integration algorithm in the vicinity of the impact.

Sakaguchi et al. [23] investigated a method for reducing friction loss in the engine timing chain using multi-body dynamics simulation. The method known as the link-by-link model was employed in the simulation to enable representation of the behavior of each single link of the chain and its friction due to contact. A model considering fluctuations in camshaft torque and crankshaft rotational speed was created. This simulation was used to verify the detailed distribution of friction in each part of the chain system as well as the changes of friction in the time domain.

Dwyer-Joyce et al. [5] used a photo elastic stress analysis technique to determine the contact stresses in an automotive chain drive tensioner. The tensioner in normal operation is subject to high magnitude, short duration impact stresses. These stresses are known to cause surface damage, wear, and surface pitting. In order to adequately design the drive system layout, a means for stress quantification is needed. A replica tensioner was made from epoxy resin and tested in a variety of configurations. A simple model was created to relate the chain link load to the resulting tensioner subsurface stress field. This model was used to correlate the observed and predicted location of isochromatic fringes, and hence to evaluate the chain link load from the photo elastic fringe pattern. Once the load was determined the contact model was used to determine the magnitude and location of the resultant peak stresses. Measured impact stresses were several times higher than those calculated from a static analysis.

Weber et al. [26], developed the new test method to facilitate the direct measurement of the real timing chain load under all engine conditions. The measuring principle was based on a strain gauged chain link in combination with a telemetric transducer system. It allowed the continuous observation of the link force during the complete chain revolution in order to identify significant dynamic effects, which are responsible for noise, wear and incorrect valve timing.

Maile et al. [10] used a design for reliability methodology based on the DfSS DCOV process for the development of a cost-effective timing chain drive. The CAE model for

the timing chain drive was used to study the distribution of the chain loads, which provided an essential input both for the concept selection stage and for the development of a reliability model for the timing chain. The DoE study on the CAE model aimed at investigating the significant factors for chain load variability lead to a reliability improvement achieved by reducing the variability in the chain load through revising the tolerances for the sprocket tooth profile. CAE tools and FEA techniques were used for computing chain loads.

Takagishi and Nagakubo [24] showed, that using the longitudinal model the load prediction accuracy was inadequate. Accordingly, a link-by-link model was created, allowing transversal vibration to be considered. As a result, the features of a chain system using a blade tensioner were clarified, thus enabling the chain load and behavior to be predicted with a higher degree of accuracy than before.

Du et al. [4] developed a MBS model of the balancer chain drive. Such a model included a crank train system coupled to a full balancer drive system including the chain drive, balance shafts, and water pump. The nonlinear stiffness and damping effects of the baseline compliant crank chain sprocket and its design iterations were added to the model to understand the basic characteristics and find an optimal setup for the engine start-up period.

### **3. Lubricants with SiO<sub>2</sub> nanoparticles**

Some studies related to the effect of addition of SiO<sub>2</sub> nanoparticles into lubricating oil on its tribological features.

Rashed & Nabhan [21] studied tribological behavior of mineral 20W-50 and semi-synthetic 15W-50 oil dispersing by different amounts (0.5 and 1.0%wt. oil) of SiO<sub>2</sub> nanoparticles. Experiments were carried out on tribometer test-rig under normal load at different temperature values from range 40°C to 100°C. The addition of SiO<sub>2</sub> to engine oils had not reduced the friction coefficient to a great extent.

Li et al. [9] dispersed ultrasonically 0.3 wt.% of SiO<sub>2</sub> nanoparticles in ST5W/30 mobile oil. Such a nano-lubricant was investigated on a reciprocating tribotester and a four-ball tribotester. As a result, the frictional coefficient decreased in relative to pure ST5W/30 gas mobile oil.

Peng et al. [18] reported, that the SiO<sub>2</sub> nanoparticles oleic dispersed in acid exhibited the similar tribological behavior as diamond nanoparticles in liquid paraffin. During friction the micro-grooves were formed, and then more spherical nanoparticles rolled into the contact area like tiny bearing, balls which reduce the sliding friction.

Nabhan & Rashed [13] studied tribological behavior of two types of lubricant oils dispersing by different amount of SiO<sub>2</sub> and TiO<sub>2</sub> nanoparticles. Experiments were carried out using tribometer test-rig under normal load at different temperatures, 40°C, 80°C and 100°C. The concentrations of Nano oxides additives that used are 0.5% and 1.0% wt. The lowest value of the friction coefficient and wear rate achieved for mineral and semi synthetic lubricant oils with adding 1.0% wt. of TiO<sub>2</sub> at 80°C and 100°C, respectively. The adding SiO<sub>2</sub> to engine oils played only a small role in reducing the friction coefficient.

Prabu et al. [20] studied the tribological characteristics of the commercial SN lubricating oil with addition of SiO<sub>2</sub> nanoparticles. Wear tests were conducted on plain oil and

oil with nanosized SiO<sub>2</sub> additives using a four ball tribotester. It was obtained a considerable reduction in the values of the analyzed: wear scar diameter, wear angle and wear depth for the gear oil added with SiO<sub>2</sub> nanoparticles of 0.4 wt. %.

According to [3], SiO<sub>2</sub> nanoparticles synthesized by the sol-gel approach were engineered for size and surface properties by grafting hydrophobic chains to prevent their aggregation and facilitate their contact with the phase boundary, thus improving their dispersibility in lubricant base oils. The surface modification was performed by covalent binding of long chain alkyl functionalities using lauric acid and decanoyl chloride to the SiO<sub>2</sub> NP surface. The tribological properties of the dispersions were analyzed under extreme load conditions using a Stanhope Seta Shell Four-Ball E.P. Lubricant Tester working at 1470 rpm shaft speed. The 12.7 mm diameter tests balls with 0.035 μm roughness were made from AISI 52100 steel. The dendritic structure of the external layer allowed reducing the friction coefficient and wear.

Patil et al. [16] studied the tribological behavior of SiO<sub>2</sub> nanoparticles as additives in Paraffin based SN-500 Base oil. All tests were carried out using pin-on-disk tribotester under variable load and concentration of nanoparticles in lubricating oil. The SiO<sub>2</sub> nanoparticles added into base oil exhibited good friction reduction and anti-wear properties. The SiO<sub>2</sub> nanoparticles in the SN-500 base oil decreased friction coefficient by 61%, 55% and 43% at 0.5wt.% concentration and 36%, 76% and 17% at 0.75wt.% concentration respectively, as compared with standard base oil without SiO<sub>2</sub> nanoparticles. Such tribological behavior was affected by the deposition of nanoparticles on the rubbing surfaces.

#### **4. Modelling of chain transmission**

Some models of chain transmissions were elaborated with different level of their complexity.

Novotny and Pišteš [15] stated that computational simulation of chain drives has not been developing too long due to high demands on the computational technology. They focused on simulation of dynamics of the timing chain drive with the use of a multibody system. A mass-produced four cylinder in-line engine with two camshafts and two valves per cylinder has been used as a computational model.

According to [22], a model of roller chain and sprocket dynamics was developed, aimed at analyses of dynamic effects of chain drive systems in automotive valvetrains. Each chain link was modeled as a rigid body with planar motion, with three degrees of freedom and connected to adjacent links by means of a springs and dampers. The kinematics of roller-sprocket contacts were modeled in full detail. Sprocket motions in the chain's plane, resulting from torsional and bending motions of attached camshafts were also considered. One or two-sided guides could be treated as well as stationary, sliding or pivoting tensioners operated mechanically or hydraulically. The model also considered the contact kinematics between chain link rollers and guides or tensioners, allowing for guides/tensioners of arbitrary shape, or simpler (flat and circular) geometries. The model captured the effects of the dynamics of the chain

drive on valvetrain behavior both qualitatively and quantitatively.

According to [7], the timing chain drives simulation results is often represented as families of function graphs (data series). Previously, the analysis of those results was based on static 2D diagrams and animated 3D visualizations. They were suitable for the detailed analysis of a few simulation variants, but not for the comparison of many cases. It was proposed a new approach to the analysis based on coordinated linked views and advanced brushing features. The proposed method introduced a novel, so-called segmented curve view, which could display distributions in families of function graphs. The segmented curve view combined individual function graphs where for a fixed value of the independent variable, a bar extended from minimum to maximum values across the family of function graphs. Each bar was divided into segments (bins) with a color that represents the number of function graphs with the value in that segment.

According to [11] the optimized chain and belt drives can have similar efficiency. While chain drives have higher efficiency than dry belt drives, chain drives and wet belt drives perform similarly. A common dry belt features a strength-to-width ratio of less than half that of a similar chain application. Due to the higher strength-to-width ratio, chain systems featuring a hydraulic tensioner, tight strand guide and slack strand tensioner arm contain all the elements necessary for adapting to additional engine variants with minimal modifications. As a result, design decisions regarding timing drives should be made by considering several different criteria. Adaptability, low dynamic cam oscillation, strength and best-in-class NVH performance can make chain drives the best solution. With proven long-term field durability, chain drives offer compact packaging, optimized efficiency and robustness against dynamic instability.

Egorov et al. [6] proposed the method allowing evaluation of the efficiency of a chain drive with a high measuring frequency rate within a wide range of possible modes of operation as it used the angular acceleration and the acceleration time as controlled variables. The method used the loading rotary bodies attached to a driven shaft of a chain drive to create the rated force in a chain, eliminating a need for a loader. The method allowed determining the mechanical efficiency of chain transmissions without consideration the losses in their bearing units. Determining acceptable levels of the acceleration time of chain drives, allowed evaluation their mechanical efficiency affected by a build quality, lubrication and materials used. Such the efficiency of chain transmissions characterized degradation processes in their elements, and therefore might be a criterion of their lifetime.

Kozlov et al. [8] proposed a new approach to the evaluation of the quality of lubricants for chain transmissions, which was based on the relationship between the chain efficiency pulldown and the use of inappropriate lubricants. To control the energy efficiency of chain drives, it was applied a method using the rotary bodies with the known moments of inertia. The method allowed investigating mechanical losses in a chain drive within a wide range of

speed, load, and transient regimes of operation without the use of strain sensors. It was experimentally proved that the method allows to evaluate the quality of lubricants in the course of operation of a chain transmission.

According to [25], most of the friction in a chain drive comes from the movement of the bushings, pins and rollers. Such friction is a combination of Coulomb friction and viscous damping dependent on the lubrication. It was not included in the model presented in [25], but damping was introduced to obtain a stable solution. As most of the power is transmitted in the tight span, it was assumed that most of the damping also occurs at this side. The damping force is usually much smaller than the stretching force in the chain but is related to this. The damping force in the slack span was neglected, as the stretching force at the slack span was smaller than at the tight span. For simplicity, a viscous damping force was assumed, proportional to the relative velocity between the two end points at the tight side.

The damping force was obtained from the equation (1)

$$F_d = D_{chain} \cdot [R_{1,p} \cdot d\varphi_p / dt \cdot \cos(\varphi_{1,p} - \theta_{in,p}) - R_{1,g} \cdot d\varphi_g / dt \cdot \cos(\varphi_{1,g} - \theta_{in,g})] \quad (1)$$

The angle  $\varphi$  was used to describe the position of the sprocket (Fig. 1). The rotation coordinates to the first contacting tooth's center-line on the sprocket were  $\varphi_p$  and  $\varphi_g$  for driving and driven sprocket, respectively. To describe the position of a specific  $i$ -th roller the angle  $\varphi_i$  was used. The angles between the  $y$  axis and the first roller of each sprocket were  $\varphi_{1,p}$  and  $\varphi_{1,g}$  – for driving and driven sprocket, respectively. The angles  $\theta_{in,p}$  and  $\theta_{in,g}$  were the chain angles, relative to the  $x$  axis, of the first links in contact with the driving and driven sprocket, respectively.

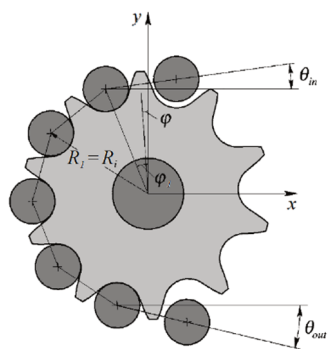


Fig. 1. Sprocket in an arbitrary load position

## 5. Materials and methods

### 5.1. Model of analyzed chain transmission

The analyzed chain transmission was one from the SI combustion engine Toyota Corolla 1.4 VVTI (Fig. 2). In the present study the model contained three assemblies:

- the assembly 1 of the crankshaft with its sprocket and its flywheel,
- the assembly 2 of the outlet camshaft with its sprocket,
- the assembly 3 of the inlet camshaft with the phaser and its sprocket, was elaborated with the Finite Element Method. The mentioned assemblies were connected through the one row chain 4.



Fig. 2. The chain transmission components

The camshaft assemblies, crankshaft assembly were treated as stiff solid bodies connected with bearings through contact elements. The crankshaft assembly rotated with constant rotational speed oftenest equal 120 rpm but for one case the full chain assembly rotated also with such a speed equal 60 rpm. The chain was modelled as the set of solid rigid components connected by contact elements. The model components allowed determining their weights and mass inertia moments.

### 5.2. Experimental stand for friction studies in the chain transmission

The friction in the chain transmission was determined using the stand utilized the original SI engine with some modifications made. The crankshaft assembly was bearing in two border mean journal bearings of crankshaft, in which the original bronze half-shells were replaced by ones made of PTFE. This was to reduce the friction coefficient between the crankshaft journals and their half-shells.

The outlet and inlet camshaft assemblies were bearing in their border pairs of journal bearings. To decrease the friction coefficient, in the bushing covers of such bearings the threaded holes were made to place grease nipples supplying lithium grease into contact zones between camshaft journals and their bushings. The grease was continuously replenished in the bearings using a grease gun.

The self-starter driving flywheel connected with camshaft was placed in the engine body through the set of screws, which was a little different than in the original vehicle. The self-starter was supplied with voltage from the battery. The chain is tensioned in real by the tensioner piston supplied by the oil pressure and acting on swingable guide. However, in the stand the piston with top plane is replaced by the piston with a roller. The position of the latter can be changed manually, what allowing quick disconnection of the front piston plane from the pressing guide.

The crankshaft and camshaft subassemblies were consecutively dismantled from the engine for replacing the sprocket on the pulley or rearranging planed components in the given assembly and re-mounted in the engine for further testing.

### 5.3. The determination of total friction torque in the chain transmission

The total friction torque in chain transmission was determined in several steps.

First, the crankshaft subassembly was arranged to be with the flywheel and with sprocket. Its mass inertia moment was equal  $I_1$ . The crankshaft subassembly was driven by self-starter to the predetermined rotational speed of 120 rpm and then braked by the friction torque  $M_{T1}$  occurring in two crankshaft main bearing up to stop. The time  $t_1$  of braking that assembly was obtained and registered.

Next, the crankshaft sprocket and the outlet camshaft subassembly sprocket were replaced with the pullies. Such pullies were connected by the belt tensioned by the roller of the tensioner piston. The crankshaft assembly was driven by the self-starter to the rotational speed of 120 rpm and, via the belt tensioned by the tensioner roller, the outlet camshaft subassembly was also driven. The mass inertia moment of the outlet camshaft assembly with its pulley was equal to  $I_2 + I_{20}$ . The contact pressure between the roller and the belt was removed via manual displacement of the roller relative to the belt and as a result the outlet camshaft subassembly was braked by the friction torque  $M_{T20}$  occurring in its two bearing up to stop. The time  $t_2$  of braking that assembly was obtained and registered.

Then the procedure was repeated for the outlet camshaft subassembly containing its pulley connected with its sprocket through additional screws. The mass inertia moment of the outlet camshaft subassembly containing its pulley and sprocket was equal to  $I_2 + I_{20} + I_{21}$ . The time  $t_3$  of braking that assembly by the friction torque  $M_{T201}$  occurring in its two bearing up to stop was obtained and registered.

Next, the procedure was repeated for the inlet camshaft assembly first containing the phaser and the sprocket connected with the pulley based on the phaser outer cylindrical surface. The mass inertia moment was equal  $I_3 + I_{30}$ . The time  $t_4$  of braking that assembly by the friction torque  $M_{T30}$  occurring in its two bearing up to stop was obtained and registered. In the following step, the procedure was repeated for the inlet camshaft assembly containing the phaser, and the sprocket connected with the pulley, which was based on the phaser outer cylindrical surface and connected with the additional heavy ring through additional screws. The mass inertia moment was equal  $I_3 + I_{30} + I_{31}$ . The time  $t_5$  of braking that assembly by the friction torque  $M_{T301}$  occurring in its two bearing up to stop was obtained and registered.

Then the angular decelerations  $\varepsilon_1, \varepsilon_2, \varepsilon_3, \varepsilon_4, \varepsilon_5$  were obtained from the equations (2)–(6) and the inertia moments were determined from the equations (7)–(11).

$$\varepsilon_1 = \omega_0 / t_1 \quad (2)$$

$$\varepsilon_2 = \omega_0 / t_2 \quad (3)$$

$$\varepsilon_3 = \omega_0 / t_3 \quad (4)$$

$$\varepsilon_4 = \omega_0 / t_4 \quad (5)$$

$$\varepsilon_5 = \omega_0 / t_5 \quad (6)$$

$$M_{T1} = I_1 \cdot \varepsilon_1 \quad (7)$$

$$M_{T20} = (I_2 + I_{20}) \cdot \varepsilon_2 \quad (8)$$

$$M_{T201} = (I_2 + I_{20} + I_{21}) \cdot \varepsilon_3 \quad (9)$$

$$M_{T30} = (I_3 + I_{30}) \cdot \varepsilon_4 \quad (10)$$

$$M_{T301} = (I_3 + I_{30} + I_{31}) \cdot \varepsilon_5 \quad (11)$$

Finally, the self-starter drove up to the predetermined crankshaft rotational speed the full assembly containing subassembly of crankshaft with flywheel and sprocket and inlet camshaft subassembly with original phaser and sprocket and the outlet camshaft subassembly with the original sprocket connected through original chain mating with its guides and tensioned by the modified tensioner piston. Then self-starter was turned off and the full assembly was braked up to stop by the friction torques:  $M_{T1}$  in two crankshaft bearings,  $M_{T21}$  in two outlet camshaft bearings,  $M_{T3}$  in two inlet camshaft bearings, respectively and the  $M_{int1}$ ,  $M_{int2}$  and  $M_{int3}$  friction torques occurred in three groups of segments of the chain transmissions (Fig. 3). The time  $t_6$  of braking the chain assembly was obtained and registered. The angular deceleration  $\varepsilon_6$  was obtained from the equation (12).

$$\varepsilon_6 = \omega_0 / t_6 \quad (12)$$

It was assumed for each case of calculations, that the friction coefficients  $\mu_a$  and  $\mu_b$  in the border bearings ‘a’ and ‘b’ were constant.

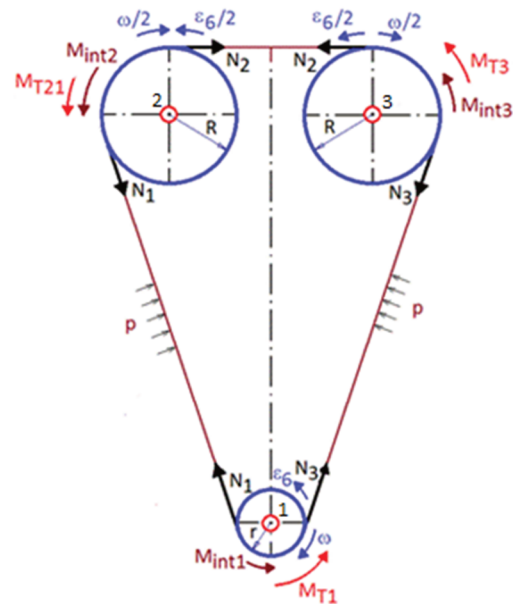


Fig. 3. The model of loading the chain transmission components

The reactions  $R_{a3s}$ ,  $R_{b3s}$  and the friction torque  $M_{T3}$  were determined using the equations (13)–(15) and the model of loading the bearings in the assembly, the total weight of which was a sum of the inlet camshaft weight  $G_3$  and the weight  $G_{3s}$  of the phaser – sprocket subassembly (Fig. 4a). Additionally, the reactions  $R_{a30}$ ,  $R_{b30}$  and the friction torque  $M_{T30}$  were determined using the equations (16)–(18) and the model of loading the border bearings in the assembly, the total weight of which was a sum of the inlet camshaft weight  $G_3$ , the weight  $G_{3s}$  of the phaser – sprocket subassembly and the weight  $G_{30}$  of the pulley embedded on the outer cylinder surface of the phaser (Fig. 4b). Also the reactions  $R_{a301}$ ,  $R_{b301}$  and the friction torque  $M_{T301}$  were determined using the equations (19)–(21) and the model of loading the border bearings in the assembly, the total weight of which was sum of the inlet camshaft weight  $G_3$ ,

the weight  $G_{3s}$  of the phaser – sprocket subassembly, the weight  $G_{30}$  of the pulley and the weight  $G_{31}$  of the heavy ring connected to the pulley (Fig. 4c). From equations (10)–(11) and (16)–(21), the friction coefficients  $\mu_a$  and  $\mu_b$  were determined. Then, the friction torque  $M_{T3}$  was obtained from equations (13)–(15).

The reactions  $R_{a21}$ ,  $R_{b21}$  and the friction torque  $M_{T21}$  were determined using the equations (22)–(24) and the model of loading the bearings in the assembly, the total weight of which was a sum of the outlet camshaft weight  $G_2$  and the weight  $G_{21}$  of the sprocket (Fig. 4d).

$$R_{a3s} + R_{b3s} = G_3 + G_{3s} \quad (13)$$

$$R_{a3s} \cdot (a + b) - G_3 \cdot b + G_{3s} \cdot c = 0 \quad (14)$$

$$M_{T3} = R_{a3s} \cdot \mu_a \cdot R_B + R_{b3s} \cdot \mu_b \cdot R_B \quad (15)$$

$$R_{a30} + R_{b30} = G_3 + G_{30} \quad (16)$$

$$R_{a30} \cdot (a + b) - G_3 \cdot b + G_{30} \cdot c = 0 \quad (17)$$

$$M_{T30} = R_{a30} \cdot \mu_a \cdot R_B + R_{b30} \cdot \mu_b \cdot R_B \quad (18)$$

$$R_{a301} + R_{b301} = G_3 + G_{30} + G_{31} \quad (19)$$

$$R_{a301} \cdot (a + b) - G_3 \cdot b + (G_{30} + G_{31}) \cdot c = 0 \quad (20)$$

$$M_{T301} = R_{a301} \cdot \mu_a \cdot R_B + R_{b301} \cdot \mu_b \cdot R_B \quad (21)$$

$$R_{a21} + R_{b21} = G_2 + G_{21} \quad (22)$$

$$R_{a21} \cdot (a + b) - G_2 \cdot b + G_{21} \cdot c = 0 \quad (23)$$

$$M_{T21} = R_{a21} \cdot \mu_a \cdot R_B + R_{b21} \cdot \mu_b \cdot R_B \quad (24)$$

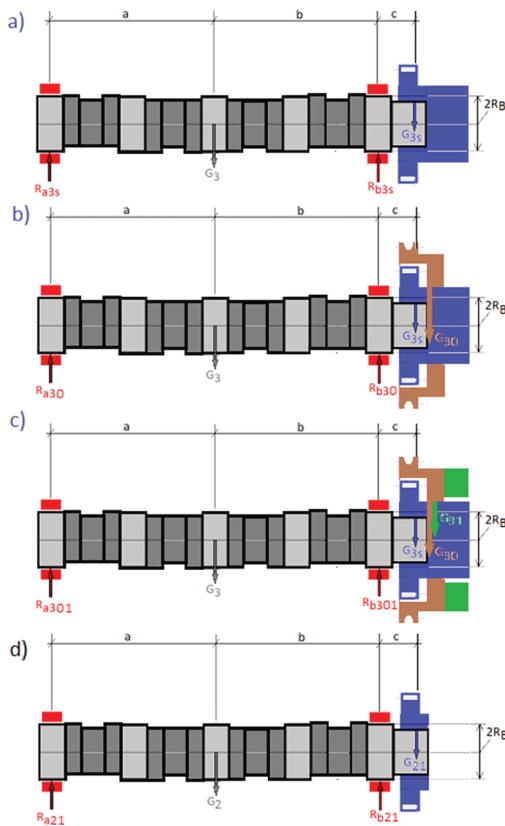


Fig. 4. Model for loading the bearing in the assembly containing: a) inlet camshaft, phaser and sprocket, b) inlet camshaft, phaser, sprocket and pulley, c) inlet camshaft, phaser, sprocket, pulley and heavy ring, d) outlet camshaft and sprocket

The internal friction torque  $M_{int}$  in the chain transmission was estimated using the scheme in the Figure 1 and the equations (25)–(36). It was assumed, that such torque contains three components:  $M_{int1}$  – related to the chain resistance to motion occurring in the crankshaft sprocket vicinity,  $M_{int2}$  – related to the chain resistance to motion occurring in the outlet camshaft sprocket vicinity, and  $M_{int3}$  – related to the chain resistance to motion occurring in the inlet camshaft sprocket vicinity.

It was also assumed, that such components are equal  $M_{int0}$ . The friction torques in the crankshaft bearing  $M_{T1c}$ , in the outlet camshafts bearing  $M_{T21c}$  and in the inlet camshaft bearing  $M_{T3c}$  during breaking of the studied full chain transmission assembly can be estimated from the equations (28). In the equation (29),  $r$  was the pitch radius for the crankshaft sprocket and  $R$  was the pitch radius for the inlet camshaft sprocket and for the outlet camshaft sprocket.

$$(N_1 - N_3) \cdot r = M_{T1c} + I_1 \cdot \epsilon_6 + M_{int1} \quad (25)$$

$$(N_2 - N_1) \cdot R = M_{T21c} + (I_2 + I_{21}) \cdot (\epsilon_6 / 2) + M_{int2} \quad (26)$$

$$(N_3 - N_2) \cdot R = M_{T3c} + I_3 \cdot (\epsilon_6 / 2) + M_{int3} \quad (27)$$

$$M_{T1c} = M_{T1}, M_{T21c} = M_{T21}, M_{T3c} = M_{T3} \quad (28)$$

$$M_{T1} \cdot R / r + I_1 \cdot \epsilon_6 \cdot R / r + M_{int1} \cdot R / r + M_{T21} + (I_2 + I_{21}) \cdot (\epsilon_6 / 2) + M_{int2} + M_{T3} + I_3 \cdot (\epsilon_6 / 2) + M_{int3} = 0 \quad (29)$$

$$R / r = 2 \quad (30)$$

$$M_{int} = M_{int1} + M_{int2} + M_{int3} \quad (31)$$

$$M_{int1} = M_{int2} = M_{int3} = M_{int0} \quad (32)$$

$$M_{int} = 3 \cdot M_{int0} \quad (33)$$

$$2 \cdot M_{T1c} + 2 \cdot I_1 \cdot \epsilon_6 + 2 \cdot M_{int1} + M_{T21c} + (I_2 + I_{21}) \cdot (\epsilon_6 / 2) + M_{int2} + M_{T3c} + I_3 \cdot (\epsilon_6 / 2) + M_{int3} = 0 \quad (34)$$

$$2 \cdot M_{T1c} + 2 \cdot I_1 \cdot \epsilon_6 + (4 / 3) \cdot M_{int} + M_{T21c} + (I_2 + I_{21}) \cdot (\epsilon_6 / 2) + M_{T3c} + I_3 \cdot (\epsilon_6 / 2) = 0 \quad (35)$$

$$M_{int} = - (3 / 4) \cdot [2 \cdot M_{T1c} + M_{T21c} + M_{T3c} + 2 \cdot I_1 \cdot \epsilon_6 + (I_2 + I_{21} + I_3) \cdot (\epsilon_6 / 2)] = 0 \quad (36)$$

#### 5.4. The determination of the friction torque between chain components

The friction torque occurring between chain roller and pin was estimated experimentally. The friction between of neighboring chain segments (outer one and inner one) in each such a pair was neglected. It was assumed, that two rollers with two inner segments create one rigid body and two pins with two outer segments create the other rigid body. The friction torque was measured using the concept of the physical pendulum.

Before measurement the chain was placed in the ultrasonic bath for the 3 min to remove the residual particles of lubricant existing in the contact zones between rollers and pins of the chain.

Then one chain pin is fixed, and the chain segments swing relative to the axis of the fixed roller. To make set of chain segments close to one rigid body, with mass inertia moment  $I_{ch}$  and weight  $m_{ch}$ , the chain segments were wrapped by several layers of foil, weight of which was neglected.

The tilts of the chain from the initial vertical position were below  $\alpha = 30$  degrees to meet the conditions of small deviations. After tilting of the chain from its initial position by  $\alpha_0 = 30$  deg, it was measured the time and number  $n$  of swingings of the pendulum up to the rest.

Then the pin was unfixed and it with the mating roller was immersed in the engine oil to introduce lubricant into contact zone between the pin and the roller and then the pin was re-fixed. Next, the measurement of the pendulum swingings was repeated.

Then the pin was once again unfixed and placed consecutively: in the kerosene, the methanol and finally in the ultrasonic bath to remove the residual particles of the pure engine oil. Next, the roller together with the pin was immersed into the engine oil with 6 wt.% amount of SiO<sub>2</sub> nanoparticles. After re-fixing of the pin, the measurement of the pendulum swingings was repeated.

The motion of the physical pendulum was described by the equation

$$I_{ch} \cdot d^2\alpha / dt^2 + \mu \cdot r_r \cdot \text{sign}(\alpha) \cdot [m_{ch} \cdot g \cdot \cos\alpha - m_{ch} \cdot r_r \cdot (d\alpha / dt)^2] = m_{ch} \cdot g \cdot l \cdot \sin\alpha \quad (37)$$

where:  $l$  – distance between the axis of fixed pin and the center of gravity of chain arranged to one rigid body,  $r_r$  – radius of chain pin,  $t$  – time,  $\mu$  – friction coefficient in the contact zone between chain roller and pin.

Integration of the equation (37) allowed estimation of friction torque in the contact between the chain pin and mating roller from the equation (38)

$$M_R = \alpha_0 \cdot m_{ch} \cdot g \cdot l / (2 \cdot n) \quad (38)$$

The angular frequency of physical pendulum swinging was estimated from the equation (39).

$$\omega = 2 \cdot \pi \cdot n / t_0 = (m_{ch} \cdot g \cdot l / I_{ch})^{0.5} \quad (39)$$

According to the equation (1), the friction between chain components is related to the speed of their motion. The internal friction torque  $M_{int}$  in the chain transmission is also related to the friction torque  $M_r$  between chain rollers and pins. During operation the estimated number  $k$  of chain rolls clearly sliding against mating pins was obtained from the equation (40).

$$k = \pi \cdot (r + 2 \cdot R) / p \quad (40)$$

where:  $p$  – chain pitch.

It was assumed, that for the constant value of rotational speed  $\omega_1$  of the crankshaft, the dry internal torque  $M_{int}$  ( $M_{rdry}, \omega_1$ ) in the chain transmission is related to the dry friction torque  $M_{rdry}$  between chain roller and pin obtained using physical pendulum method according to the equation (41).

$$M_{int}(M_{rdry}, \omega_1) = A \cdot k \cdot M_{rdry} + B \cdot \omega_1 \quad (41)$$

For the same value of speed  $v$ , the relation between internal friction torque  $M_{int}(M_{roil}, v)$  in the chain transmission lubricated by the engine oil 10W-40 and the friction torque  $M_{roil}$  in contact zone between chain roller and pin lubricated with the same oil obtained using physical pendulum method can be estimated from the equation (42).

$$M_{int}(M_{roil}, \omega_1) = A \cdot k \cdot M_{roil} + B \cdot \omega_1 \quad (42)$$

For the same value of speed  $v$ , the relation between internal friction torque  $M_{int}(M_{rSiO2}, v)$  in the chain transmission lubricated by the engine oil 10W-40 with 2 wt.% amount of SiO<sub>2</sub> nanoparticles is related to the friction torque  $M_{rSiO2}$  in contact zone between chain roller and pin lubricated with the same mixture obtained using the physical pendulum method can be estimated from the equation (43):

$$M_{int}(M_{rSiO2}, \omega_1) = A \cdot k \cdot M_{rSiO2} + B \cdot \omega_1 \quad (43)$$

For two values of crankshaft rotational speed, namely  $\omega_1 = 0.12$  rad/s and  $\omega_1 = 0.06$  rad/s, two different values of the dry internal torque  $M_{int}(M_{rdry}, \omega_1)$  were determined from the equation (41) and then the constants  $A$  and  $B$  were estimated.

## 6. Results and discussions

The values of weights and mass inertia moment were presented in the Table 1. The highest weight and the mass inertia moment had the crankshaft. The weight and mass inertia moment for the inlet camshaft were higher than for the inlet one, as the inlet camshaft assembly contained the heavy phaser.

Table 1. Weights and mass inertia moments of chain transmission components

Component	Weight M	Mass inertia moment Iz against rotation axis z
–	kg	kgm <sup>2</sup>
crankshaft	11.887	0.137593
crankshaft sprocket	0.047	0.000007
outlet camshaft	2.379	0.000341
outlet sprocket	0.165	0.000168
outlet pulley	0.172	0.000188
inlet camshaft	3.822	0.001628
inlet pulley	0.733	0.000839
inlet ring	0.858	0.000993
chain	2.496	0.002049

The values of friction torque in the bearings were presented in the Table 2. The obtained values of internal dry friction torque in the chain transmission were of 26% lower than the values of friction torque in the two modified crankshaft bearings containing PTFE shells.

Table 2. Calculated values of friction torque in bearings and internal friction torque in the chain transmission

Friction torque	Values
–	Nm
$M_{T1}$	0.288174
$M_{T20}$	0.003196
$M_{T201}$	0.002835
$M_{T3}$	0.004473
$M_{T30}$	0.003758
$M_{T301}$	0.004466
$M_{int}(\omega_1 = 0.12 \text{ rad/s})$	0.169358
$M_{int}(\omega_1 = 0.06 \text{ rad/s})$	0.167130

The resulted courses of the swinging angle  $\alpha$  of the chain arranged as a physical pendulum against time  $t$  for different cases of friction occurring in the contact zone between fixed chain pin and mating chain roller, namely: dry, lubricated

with pure engine oil and with engine oil containing 2 wt.% of SiO<sub>2</sub> nanoparticles was presented in the Fig. 5.

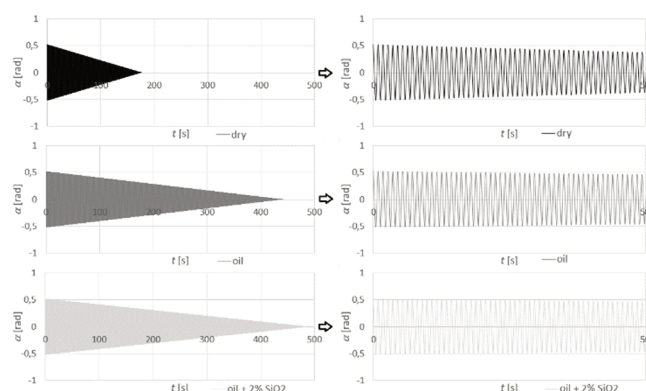


Fig. 5. The swinging angle  $\alpha$  of the chain arranged as a physical pendulum against time  $t$  for different cases of friction in the contact zone between fixed chain pin and mating chain roller: dry, lubricated with pure engine oil and with engine oil containing 2wt % of SiO<sub>2</sub> nanoparticles. Courses on the right are the increased views for courses on the left side in the figure

Table 3 presents the values of friction torque obtained from the pendulum swingings for different friction in the contact zone between fixed chain pin and chain roller mating with it. The friction torque values for the in the contact zone lubricated by the engine oil were 2.5 times lower than for the dry friction. The addition of 2 wt.% amount of SiO<sub>2</sub> nanoparticles into engine oil 10W-40 resulted in the decrease of friction torque about 10%. The constants A and B were estimated to be equal 14 and 1.22 s/m, respectively. Table 3 also included the estimated values of the internal friction torque in the chain transmissions. The value of

internal friction torque in the chain transmission lubricated by the engine oil was lower by 58% than in case of operation under the dry friction conditions. The addition of 2 wt.% amount of the SiO<sub>2</sub> nanoparticles into the engine oil decreased internal friction torque by 9% in comparison to the lubrication by pure engine oil.

Table 3. Friction torque for different friction in the contact zone

Operational conditions in contact zone	Friction torque in the contact zone between chain pin and roller	Internal friction torque in chain transmission
	Nm	Nm
Dry	0.00025	0.169326
Lubricated with engine oil	0.00010	0.070365
Lubricated with engine oil containing 2 wt.% amount of SiO <sub>2</sub> nanoparticles	0.00009	0.063768

## 7. Summary

The measurement using physical pendulum swingings method is the useful method for the estimation of friction torque in the contact zone between chain pin and roller for different lubrication conditions. The internal friction torque in the chain transmission lubricated by the engine oil can be smaller about 58% than in the case of lack of engine oil. Addition of 2 wt.% amount of the SiO<sub>2</sub> nanoparticles into the engine oil decreased internal friction torque by the 9 % in comparison to the case of engine oil without such SiO<sub>2</sub> nanoparticles.

## Nomenclature

AISI American Iron and Steel Institute  
 CAE computer aided engineering  
 DfSS design for Six Sigma  
 DoE design of experiment  
 DCOV define – characterize – optimize - verify  
 FEA finite element analysis  
 MBS multibody dynamics system

NVH noise, vibration and harshness  
 NP nano-particles  
 PTFE poli(tetrafluoroetylen)  
 SI spark ignition  
 SN synthesised  
 VVTI variable valve timing with intelligence

## Bibliography

- [1] BELMER, S., FINK, T., LORENZ, I., NEUKIRCHNER, H. Steuertriebe für Verbrennungsmotoren. Konzeption, Auslegung und Basiskonstruktion. *MTZ*. 2005, **66**(6), 466-475.
- [2] CONWELL, J.C., JOHNSON, G.E. Design, construction and instrumentation of a machine to measure tension and impact forces in roller chain drives. *Mechanism and Machine Theory*. 1996, **31**(4), 525-531. DOI: 10.1016/0094-114X(95)00014-P
- [3] DIAZ-FAES LÓPEZ, T., FERNÁNDEZ GONZÁLEZ, A., DEL REGUERO, A. et al. Engineered silica nanoparticles as additives in lubricant oils. *Sci. Technol. Adv. Mater*. 2015, **16**, 055005 (11pp). DOI: 10.1088/1468-6996/16/5/055005
- [4] DU, H.Y.I., FANG, X., CHEN, J.-S. et al. Modelling and simulation of torsional vibration of the compliant sprocket in balance chain drive systems. *SAE International Journal of Fuels Lubrication*. 2008, **1**(1), DOI: 104271/2008-01-1529
- [5] DWYER-JOYCE, R.S., LEWIS, R., WARD, A. et al. Determination of impact stresses in an automotive chain drive component. *SAE Technical Paper* 2006-01-0766. 2006. DOI: 10.4271/2006-01-0766
- [6] EGOROV, A.V., KOZLOV, K.E., BELOGUSEV, V.N., A method for evaluation of the chain drive efficiency. *Journal of Applied Engineering Science*. 2015, **13**(4), 341, 277-282. DOI: 10.5937/jaes13-9170
- [7] KONYHA, Z., MATKOVIC, K., GRACANIN, D. et al. Interactive visual analysis of a timing chain drive using segmented curve view and other coordinated views. In: Andrienko, G., Roberts J.C., Weaver C. editors. *Proceedings of the 5th International Conference on Coordinated & Multiple Views in Exploratory Visualization (CMV2007)*. IEEE Computer Society Press. July 2007, 3-15.

- [8] KOZLOV, K.E., EGOROV, A.V., BELOGUSEV, V.N. Experimental evaluation of chain transmissions lubricants quality using a new method based on additional inertia moment use. *International Conference on Industrial Engineering, ICIE 2017. Procedia Engineering*. 2017, **206**, 617-623. DOI: 10.1016/j.proeng.2017.10.526
- [9] LI, X., CAO, Z., ZHANG, Z. et al. Surface-modification in situ of nano-SiO<sub>2</sub> and its structure and tribological properties. *Appl. Surf. Sci.* 2006, **252**, 7856-7861. DOI: 10.1016/j.apsusc.2005.09.068
- [10] MAILE, K., CAMPEAN, F., DAY, A. Design for reliability of an engine timing chain. *SAE Technical Paper* 2009-01-0206. DOI: 10.4271/2009-01-0206
- [11] MOSTER, A., GOODROW, J. Timing chains or belts? Tests reveal which is more efficient. *Borg Warner Knowledge Library*. 2014.
- [12] MULIK, A.V., GUJAR, A.J. Literature review on simulation and analysis of timing chain of an automotive engine. *Int. Journal of Engineering Research and Application*. 2016, **6**(8), (Part 1), 17-21.
- [13] NABHAN, A., RASHED, A. Effects of TiO<sub>2</sub> and SiO<sub>2</sub> nano additive to engine lubricant oils on tribological properties at different temperatures. *20th International Conference on Aerospace, Mechanical, Automotive and Materials Engineering (ICAMAME2018)*. Rome 2018.
- [14] NOVOTNÝ, P., PÍŠTĚK, V. Dynamics of chain timing drive. In: *Opořebení spolehlivost diagnostika 2008*. Brno: Vydavatelské oddělení UO, Brno, 2008, 137-143.
- [15] NOVOTNÝ, P., PÍŠTĚK, V. Virtual prototype of timing chain drive. *Engineering Mechanics*. 2009, **16**(2), 123-130.
- [16] PATIL, H.H., CHAVAN, D.S., PISE, A.T. Tribological properties of SiO<sub>2</sub> nanoparticles added in SN-500 base oil. *International Journal of Engineering Research & Technology (IJERT)*. 2013, **2**(5), 763-768.
- [17] PEDERSEN, S.L. Simulation and analysis of roller chain drive systems. Ph.D. thesis, Department of Mechanical Engineering, Solid Mechanics, Technical University of Denmark 2004.
- [18] PENG, D.X., KANG, Y., HWANG, R.M. et al. Tribological properties of diamond and SiO<sub>2</sub> nanoparticles added in paraffin. *Tribol. Int.* 2009, **42**, 911-917. DOI: 10.1016/j.triboint.2008.12.015
- [19] PEREIRA, C., AMBRÓSIO, J., RAMALHO, A. Contact mechanics in a roller chain drive using a multibody approach. *11th Pan-American Congress of Applied Mechanics January 04-08, 2010*, Foz do Iguaçu, PR, Brazil.
- [20] PRABU, K., NALINI, B., SURESH, B. et al. Analysis of tribological properties of lubricating gear oil with nano silica particles. *Journal of Achievements in Materials and Manufacturing Engineering*. 2016, **79**(2), 59-65.
- [21] RASHED, A., NABHAN, A. Influence of adding nano graphene and hybrid SiO<sub>2</sub>-TiO<sub>2</sub> nano particles on tribological characteristics of polymethyl methacrylate (PMMA). *KGK – Kautschuk Gummi Kunststoff*. 2018, **71**(11-12), 32-37.
- [22] RODRIGUEZ, J., KERIBAR, R., FIALEK, G. A comprehensive drive chain model applicable to valvetrain systems. *SAE Technical Paper* 2005-01-1650. 2005. DOI: 10.4271/2005-01-1650.
- [23] SAKAGUCHI, M., YAMADA, S., SEKI, M. et al. Study on Reduction of Timing Chain Friction Using Multi-Body Dynamics, *SAE Technical Paper* 2012-01-0412, DOI: 10.4271/2012-01-0412
- [24] TAKAGISHI, H., NAGAKUBO, A. Multi-body dynamic chain system simulation using a blade tensioner. *SAE Technical Paper* 2006-32-0067. 2006. DOI: 10.4271/2006-32-0067
- [25] TROEDSSON, I., VEDMAR, L. A method to determine the dynamic load distribution in a chain drive. *Proc Instn Mech Engrs*. 2001, **215**, Part C, 569-579. DOI: 10.1243/0954406011520959
- [26] WEBER, C., HERRMANN, W., STADTMANN, J. Experimental investigation into the dynamic engine timing chain behaviour. *SAE Technical Paper* 980840. 1998. DOI: 10.4271/980840

Edward Spinache – Faculty of Economic and Industrial Engineering, University of Pitesti, Romania.  
e-mail: [eddy96261@gmail.com](mailto:eddy96261@gmail.com)



Marek Wozniak, DEng. – Department of Vehicles and Fundamentals of Machine Design, Lodz University of Technology.  
e-mail: [marek.wozniak@p.lodz.pl](mailto:marek.wozniak@p.lodz.pl)



Adrian Trandafir – Faculty of Economic and Industrial Engineering, University of Pitesti, Romania.  
e-mail: [trandafir\\_adrian31@yahoo.com](mailto:trandafir_adrian31@yahoo.com)



Przemyslaw Kubiak, DSc., DEng. – Department of Vehicles and Fundamentals of Machine Design, Lodz University of Technology.  
e-mail: [przemyslaw.kubiak@p.lodz.pl](mailto:przemyslaw.kubiak@p.lodz.pl)



Mihai Diaconu – Faculty of Mechanics and Technology, University of Pitesti, Romania.  
e-mail: [mihai.diaconu23@yahoo.com](mailto:mihai.diaconu23@yahoo.com)



Krzysztof Siczek, DSc., DEng. – Department of Vehicles and Fundamentals of Machine Design, Lodz University of Technology.  
e-mail: [ks670907@p.lodz.pl](mailto:ks670907@p.lodz.pl)



Prof. Gustavo Ozuna – Department of Industrial Engineering and Systems, University of Sonora, Mexico.  
e-mail: [gozuna@industrial.uson.mx](mailto:gozuna@industrial.uson.mx)

